Synthesis of Monolithic Porous Carbon Aerogels Without Use of Supercritical Fluid Drying from Polymer-Crosslinked Xerogel Powders

Daniel Greenan
Faculty Advisor: Chariklia Sotiriou-Leventis
Department: Chemistry

March 30, 2021

Abstract:

Carbon aerogels are well known for their high surface areas and high porosities, which are used for CO_2 capture, gas-separations, electrochemical cells, catalysis, etc. They are typically made from pyrolysis of a variety of carbonizable polymeric aerogels, which in turn are synthesized via sol-gel methods. Synthesis of those aerogels involve supercritical-fluid drying of wet-gels by replacing the pore-filling solvent with liquid CO_2 that can be vented off as a gas, which allows the pores to retain their shape. We propose an alternative route for the synthesis of carbon aerogels from xerogel powders, which allows to speed-up the solvent exchange process and bypasses the supercritical fluid drying resulting in time and energy efficient methodology for fabricating porous carbons. These xerogel powders are compressed into different shapes, pyrolyzed and etched with hydrofluoric acid and/or CO_2. At best, these monolithic porous carbons have high surface areas of 1547 m^2/g and porosities of 77%.

Introduction:

Carbon aerogels are well known for their high surface areas and high porosities. Their applications have been demonstrated in a wide range of areas such as CO_2 capture, gas separations, electrochemical cells, catalysis, etc (1,2). They are typically made from pyrolysis of a variety of carbonizable polymeric aerogels, which in turn are synthesized via sol-gel methods. Synthesis of those aerogels involve supercritical fluid drying of wet-gels by replacing the pore-filling solvent with liquid CO_2 that can be vented off as a gas, which allows the pores to retain their shape (3). Thus, the high porosity of carbon aerogels is derived from both the innate porosity of the precursor polymeric aerogels, and the porosity created during pyrolysis of those aerogels. In contrast, here an alternative route is proposed for the synthesis of carbon aerogels from xerogel powders, which allows to speed-up the solvent exchange process and bypasses the supercritical fluid drying resulting in a time and energy efficient methodology for fabricating porous carbons.

In this new method, cross-linked silica xerogel powder will be prepared via free-radical surface-initiated polymerization of acrylonitrile (AN) on the network of tetramethoxysilane (TMOS)-derived silica suspension. The reaction involved in the synthesis of polyacrylonitrile cross-linked silica (PAN@TMOS) is shown in Scheme 1. Additionally, cross-linked silica xerogel powder will be prepared via conformal nano thin coating layer of carbonizable polyurea (PU) derived from the reaction of an aromatic triisocyanate TIPM (triisocyanatophenyl methane) with –OH, $–NH_2$ and absorbed water on the surface of TMOS-derived silica suspension. The wet powders of PAN@TMOS and PUA@TMOS will be dried under vacuum at 80 °C to yield xerogel powders, which will be compressed into pellets using a suitable die and a hydraulic press. The pellets will then be aromatized, carbonized, and treated with hydrofluoric acid to remove SiO_2 particles creating the porosity.

Three xerogel powder formulations have been made and characterized so far; two PAN@TMOS using TMOS:APTES ratio of 90:10 (mol/mol) and different amounts of cross-linking monomer (30% and 60% AN), and one PUA@TMOS using 4x TIPM (vol/vol) of the TMOS-derived silica suspension. Future plans involve making five more different xerogel powder formulations; two PAN@TMOS using TMOS:APTES ratio of 70:30 (mol/mol) and different amounts of cross-linking monomer (30% and 60% AN), and three PUA@TMOS using 6x, 2x and 1x TIPM (vol/vol) of the TMOS-derived silica suspension and characterize the materials along the process. Additionally, based on the pore size distribution and other physical/material properties, the application of the porous carbon aerogels made via the proposed route will be demonstrated.

Experimental:

Preparation of ABCVA@silica powder. In a typical procedure, hexane (43 mL, 3 the volume of the intended sol) was added under flowing dry (drying tube) Ar (99.99999%) to a three-neck round bottom flask equipped with a mechanical stirrer and a drying tube. To that flask, Solution A consisting of 4.5 mL of CH_3OH and 3.85 mL (0.0260 mol) of TMOS, and solution B consisting of 4.5 mL of CH_3OH, 1.5 mL (0.0830 mol) of water and 40 μL NH_4OH were added successively at room temperature under vigorously stirring (770 – 950 rpm). As soon as the mixture developed fine particles and turned white (approximately 20 min), Solution C consisting of 0.67 mL (0.0028 mol) of APTES (TMOS:APTES = 9:1 by mol) and 0.4049g (0.0014 mol) of ABCVA (APTES:ABCVA = 2:1 by mol) dissolved in 8.70 mL anhydrous THF, was added to the flask. The reaction mixture was stirred at the same rate for 24 h at room temperature. The resulting ABCVA@silica suspension was transferred to centrifuge tubes (50 ml, Cat. no. 05-539-8, Fisher Scientific) and the solvent was exchanged once with methanol and thrice with toluene. After this solvent exchange the ABCVA@silica suspension was either processed to PAN@silica powder (see next section) or was dried under vacuum at 50 °C after three more washes with acetone. All washes and solvent exchanges were carried out with centrifugation for 15-20 min at 2450 rpm. Each time, the supernatant solvent was removed and the volume of the new solvent that was brought in was 2 the volume of the compacted slurry (paste) at the bottom of the centrifuge tubes. Before every new centrifugation step, the compacted slurry was re-suspended with vigorous agitation using Vortex-Genie (Model no. K-550-G, Scientific Industries) and a glass rod.

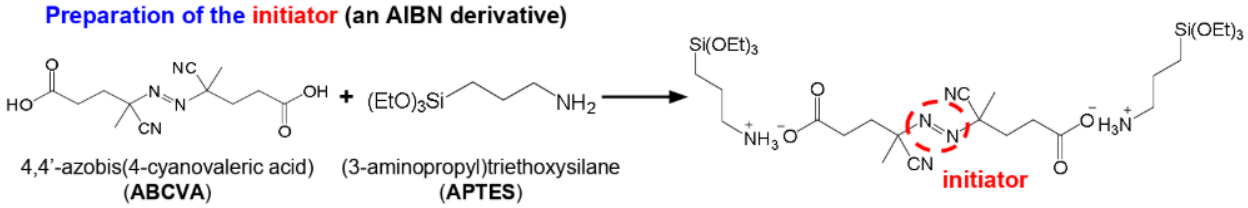

Preparation of crosslinked PAN@silica powder. In a typical procedure, 13.5 mL inhibitor free acrylonitrile in 5 mL toluene (acrylonitrile: toluene = 2.7:1 by v/v) was added in a round bottom flask containing the above obtained ABCVA@silica slurry from the toluene wash. The mixture was heated at 55°C and stirred using a magnetic stirrer at 400 rpm. At the end of the 24 h period, the mixture was allowed to cool to room temperature and then the slurry was centrifuged for 15 to 20 min followed successively by three toluene washes and three acetone washes. Always, the wash solvent was removed by centrifugation (11). Again, for all washes, the volume of solvent added was twice the volume of the paste at the bottom of the tubes. After removing the solvent from the last acetone wash, the contents of the tubes were transferred with the aid of small portions of acetone and were combined in a round bottom flask. Acetone was removed and the product was dried under reduced pressure (water aspirator connected via a drying tube) at 50°C into a dry, freely flowing PAN@silica powder.

Scheme 1: Synthesis of PAN@TMOS suspension:

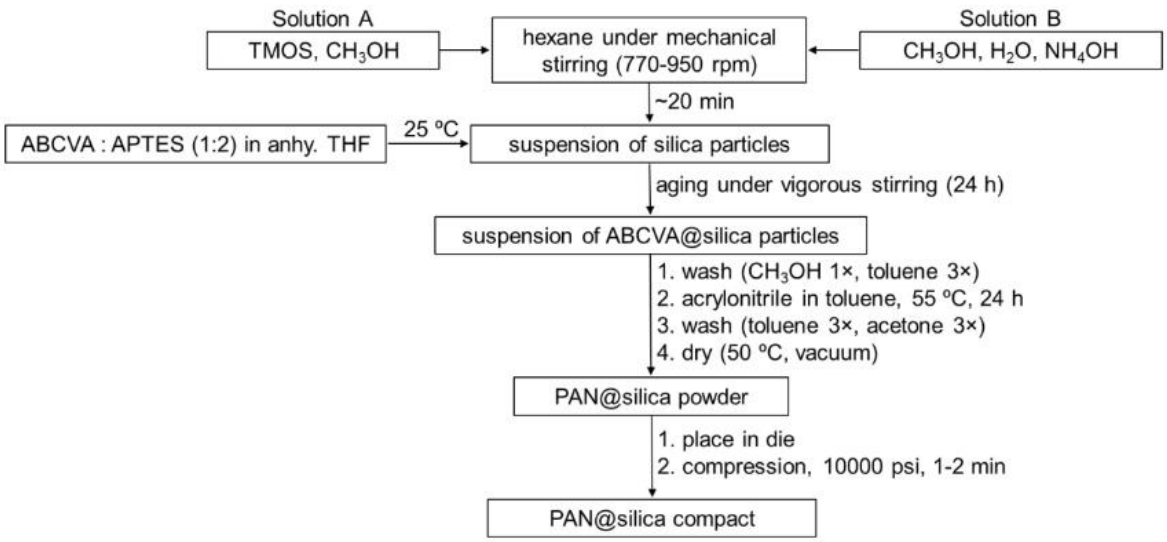

Formulations of crosslinked PAN@silica powder. Two alternate formulations were made of this PAN@silica powder. In the first alternate formulation, a 70:30 TMOS to APTES mole ratio was used with a 60% acrylonitrile crosslinking agent. 430mL of hexane was added under flowing dry argon to a three-neck round bottom flask equipped with a mechanical stirrer and a drying tube. Solution A consisted of 45mL of CH_3OH and 30.10mL (0.2022 mol) of TMOS, and solution B consisted of 45mL of CH_3OH, 15mL of water, and 400µL of NH_4OH. Solution C consisted of 160mL of THF, 12.1217g (0.04332mol) of ABCVA, and 20.28mL of APTES. In the second alternate formulation, a 70:30 TMOS to APTES mole ratio was used with a 30% acrylonitrile crosslinking agent, so solutions A, B, and C had the same content as the first alternate formulation above.

Preparation and processing of PAN@silica compacts. Dry PAN@silica powder was compressed into various cylindrical monolithic objects using stainless steel die and a hydraulic press operated at 10,000 psi. Placement of the powder in the die was carried out in small portions under continuous tapping. Compressed PAN@silica compacts were then converted to aromatized-PAN@silica compacts pyrolytically in a tube furnace at 300℃ for 24 h under flowing O_2. The gas flow was always set at 325mL min^{-1}. These aromatized-PAN@silica compacts were then converted to C-PAN@silica compacts pyrolytically in a tube furnace at 800℃ for 5 h under flowing ultrahigh purity argon. The gas flow was always set at 325 mL min^{-1}. These C-PAN@silica compacts are then processed via two processing routes as shown in the Scheme 2. HF etching was carried out in a HDPE vial (20mL, Cat. no. 03-337-23, Fisher Scientific) with a rubber septum on it under reduced pressure (using water aspirator). CO_2 etching was carried out in a tube furnace at 1000°C for 3 h under flowing CO_2. The gas flow was always set at 325 mL min^{-1}.

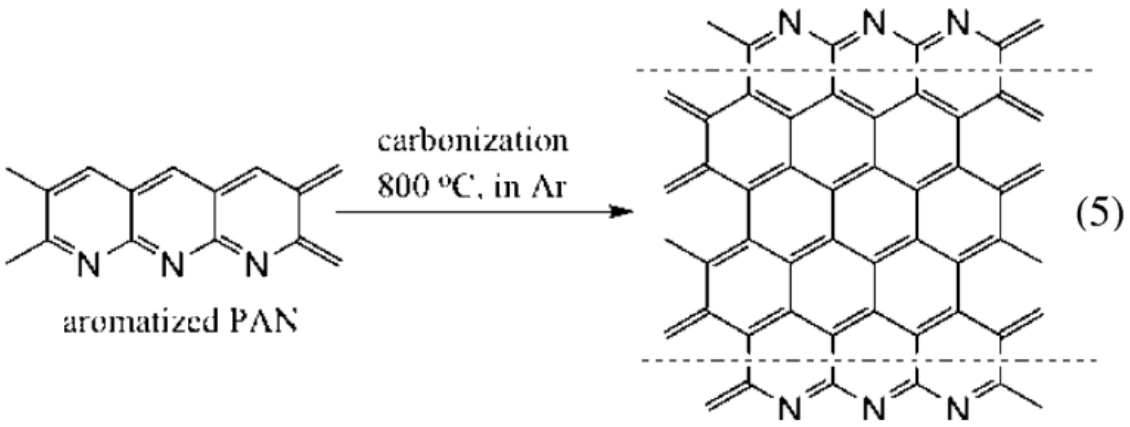

(5)

Scheme 2: Various processing steps of PAN@silica compact

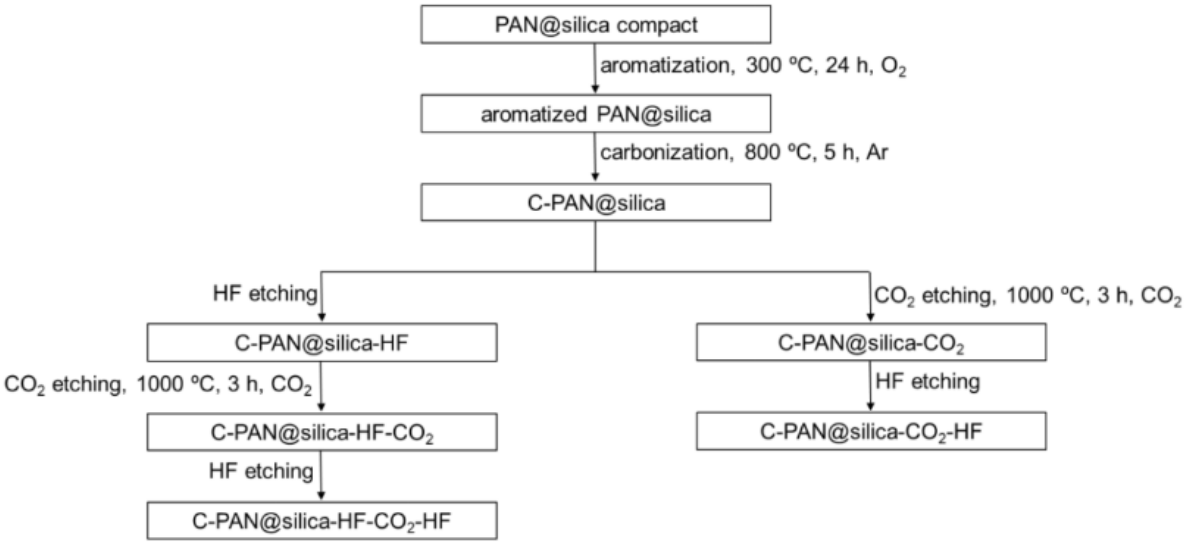

Preparation of APTES@TMOS silica powder. Hexane (43 mL, 3 the volume of the intended sol) was added under flowing dry (drying tube) argon (99.99999%) to a three-neck round bottom flask equipped with a mechanical stirrer and a drying tube. To that flask, Solution A consisting of 4.5 mL of CH_3OH and 3.85 mL (0.026 mol) of TMOS, and solution B consisting of 4.5 mL of CH_3OH, 1.5 mL (0.083 mol) of water and 40 μL NH_4OH were added successively at room temperature under vigorously stirring (770 - 950 rpm). As soon as the mixture developed fine particles and turned white (approximately 20 min), 1.28 mL of APTES (approximately 1/3 the volume of TMOS) was added to the flask, and the reaction mixture was stirred at the same rate for 24 h at room temperature. The resulting APTES@TMOS suspension was transferred to centrifuge tubes (50 ml Fisher Scientific) and the solvent was exchanged twice with ethyl acetate and once with water-saturated ethyl acetate (EtOAc/H_2O). After standing for 15 h in EtOAc/H_2O, the APTES@TMOS suspension was either processed to PUA@silica powder (see

next section) or was dried under vacuum at 50°C. All washes and solvent exchanges were carried out with centrifugation for 15-20 min at 2450 rpm. Each time, the supernatant solvent was removed and the volume of the new solvent that was brought in was two times the volume of the compacted slurry (paste) at the bottom of the centrifuge tubes. Before every new centrifugation step, the compacted slurry was re-suspended with vigorous agitation with Vortex-Genie (Model no. K-550-G, Scientific Industries) and a glass rod.

Formulation of APTES@TMOS silica powder. Two alternate formulations were made of this APTES@TMOS silica powder. In these formulations, there was one that was crosslinked with a TIPM solution that was 2 times the volume of the APTES@TMOS slurry, and the other formulation had one times the volume of the APTES@TMOS slurry.

Scheme 3. Two routes to a common product: Silica gels surface modified with APTES

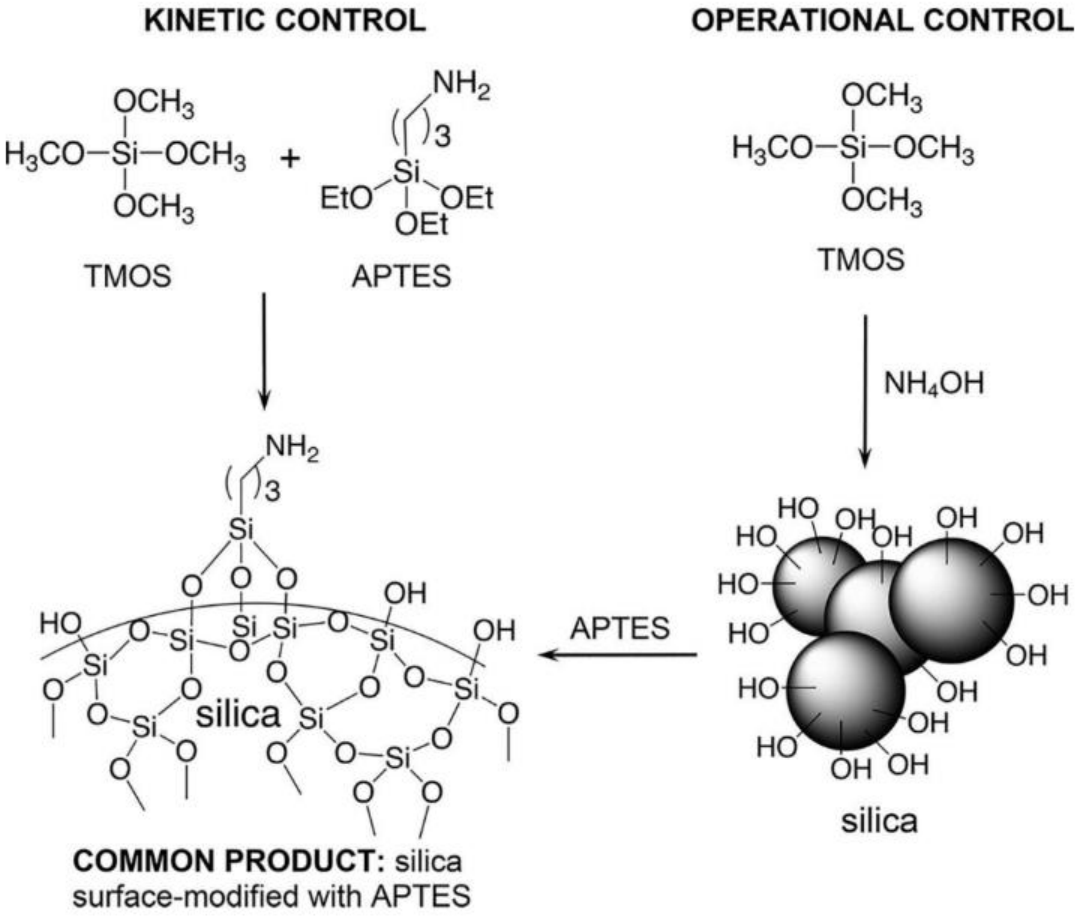

Preparation of crosslinked PUA@silica powder. In a typical procedure, TIPM solution as received (four times the volume of the centrifuged paste) was added to the centrifuge tubes containing the APTES@TMOS slurry from the last EtOAc/H_2O wash, the tubes were sealed tightly with their caps, and the suspension was heated in an oven at 65°C for 72 h (34). The mixture was swirled slowly every 10 to 12 h to re-distribute the settled powder and increase the

diffusion rate. At the end of the 3-day period, the tubes were allowed to cool to room temperature, and they were centrifuged for 15 to 20 min followed successively by three ethyl acetate washes. Always, the wash solvent was removed by centrifugation. Again, for all washes, the volume of solvent added was twice the volume of the paste at the bottom of the tubes. After removing the solvent from the last ethyl acetate wash, the contents of the tubes were transferred with the aid of small portions of ethyl acetate and were combined in a round bottom flask. Ethyl acetate was removed, and the product was dried under reduced pressure (water aspirator connected via a drying tube) at 55°C into a dry, freely flowing PUA@silica powder.

Scheme 4. Crosslinking skeletal silica nanoparticles (Native or –NH2 modified) with a Triisocyanate (TIPM)

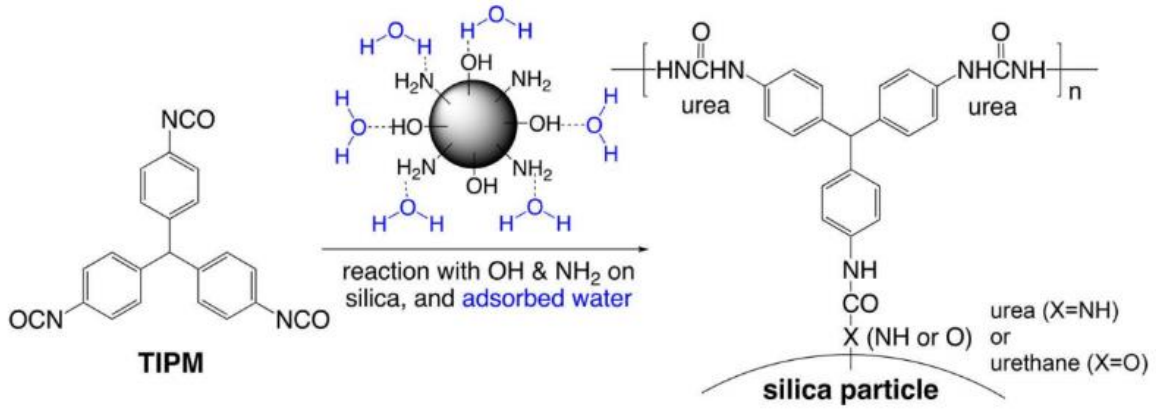

Preparation and processing of PUA@silica compacts. Dry PUA@silica powder was compressed into various cylindrical monolithic objects using stainless steel die and a hydraulic press operated at 10,000 psi. Placement of the powder in the die was carried out in small portions under continuous tapping. Compressed PUA@silica compacts were then converted to C-PUA@silica compacts pyrolytically in a tube furnace at 800 °C for 5 h under flowing ultrahigh purity argon. The gas flow was always set at 325 mL min^{-1}. These C-PUA@silica compacts are processed via two processing routes as shown in the Scheme 5. HF etching was carried out in a HDPE vial (20mL, Cat. No. 03-337-23, Fisher Scientific) with a rubber septum on it under reduced pressure (using water aspirator). CO_2 etching was carried out in tube furnace at 1000°C for 3 h under flowing CO_2. The gas flow was always set at 325 mL min^{-1}.

Scheme 5: Various processing steps of PUA@silica compacts

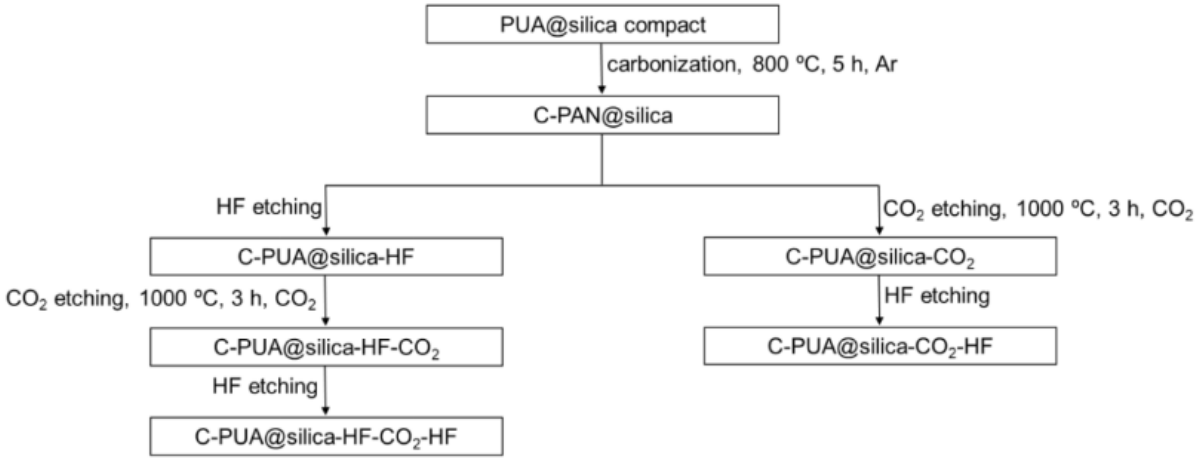

Methods. Pyrolytic conversion of PAN@silica compacts and PUA@silica compacts to their respective processed compacts was carried out in a programmable MTI GSL1600X-80 tube furnace (outer and inner tubes both of 99.8% pure alumina; outer tube: 1022 mm × 82 mm × 70 mm; inner tube: 610 mm × 61.45 mm × 53.55 mm; heating zone at set temperature: 457 mm). The temperature of the tube furnace was raised under flowing O_2, argon or CO_2 from ambient to the carbothermal reaction temperature at 2.5°C min^{-1}. The temperature was maintained at that level for the prescribed length of time. Cooling back to room temperature was carried out under constant flow of O_2, Ar, or CO_2, again at 2.5°C min^{-1}.

Physical Characterization. Bulk densities (ρb) were calculated from the weight and the physical dimensions of the samples. Skeletal densities (ρs) were determined with helium pycnometry using a Micromeritics AccuPyc II 1340 instrument. Samples for skeletal density measurements were outgassed for 24 h at 80°C under vacuum before analysis. Percent porosities, Π, were determined from the ρb and ρs values via $\Pi = 100 \times (\rho s - \rho b)/\rho s$.

Pore Structure Analysis. BET surface areas were determined with N_2-sorption porosimetry at 77K using a Micromeritics ASAP 2020 surface area and porosity analyzer. Samples for N_2-sorption analysis were outgassed for 24 h at 80°C under a vacuum before analysis.

PUA@silica (4xTIPM by vol. crosslinked)

sample I.D.	linear shrinkage[a,b] (%)	bulk density[a], ρ_b (g cm^{-3})	skeletal density[c], ρ_s (g cm^{-3})	porosity[d], Π (% v/v)	mass loss[a], (% w/w)	specific pore volume (cm^3 g^{-1})			BET surface area[h], σ (m^2 g^{-1})	avg pore diameter[i], Φ (nm)
						V_{Total}[e]	$V_{1.7\text{-}300\ nm}$[f]	$V_{>300\ nm}$[g]		
PUA@silica compact		0.9673 ± 0.0222	1.3626 ± 0.0017	29.01%		0.30	0.08	0.22	34.9 [3.67]	34.35 [9.31]
C-PUA@silica	33.67 ± 0.21 %	1.1529 ± 0.0325	1.9534 ± 0.0206	40.98%	49.82 ± 0.21 %	0.36	0.01	0.34	3.87 [0.85]	376.20 [13.20]
C-PUA@silica-HF	34.06 ± 0.41 %	0.8354 ± 0.0534	1.7546 ± 0.0088	52.39%	65.12 ± 0.85%	0.63	0.31	0.32	762 [178]	3.29 [3.18]
C-PUA@silica-HF-CO_2	42.80 ± 1.41 %	0.5368 ± 0.0260	1.9433 ± 0.0313	72.38%	79.32 ± 1.29 %	1.35	0.40	0.95	1148 [646]	4.70 [2.93]
C-PUA@silica-HF-CO_2-HF	41.83 ± 1.93 %	0.6476 ± 0.0627	1.7869 ± 0.0062	63.76%	74.93 ± 3.68 %	0.98	0.38	0.60	911 [437]	4.32 [3.13]
C-PUA@silica-CO_2	44.09 ± 0.87 %	1.0362 ± 0.0132	2.1541 ± 0.0071	51.90%	65.28 ± 1.53 %	0.50	0.09	0.41	731 [368]	2.74 [2.33]
C-PUA@silica-CO_2-HF	44.15 ± 1.61 %	0.5576 ± 0.0346	1.8455 ± 0.0286	69.79%	80.68 ± 3.03 %	1.25	0.64	0.61	1032 [394]	4.85 [3.65]

N_2 sorption for PUA@silica processed pellets

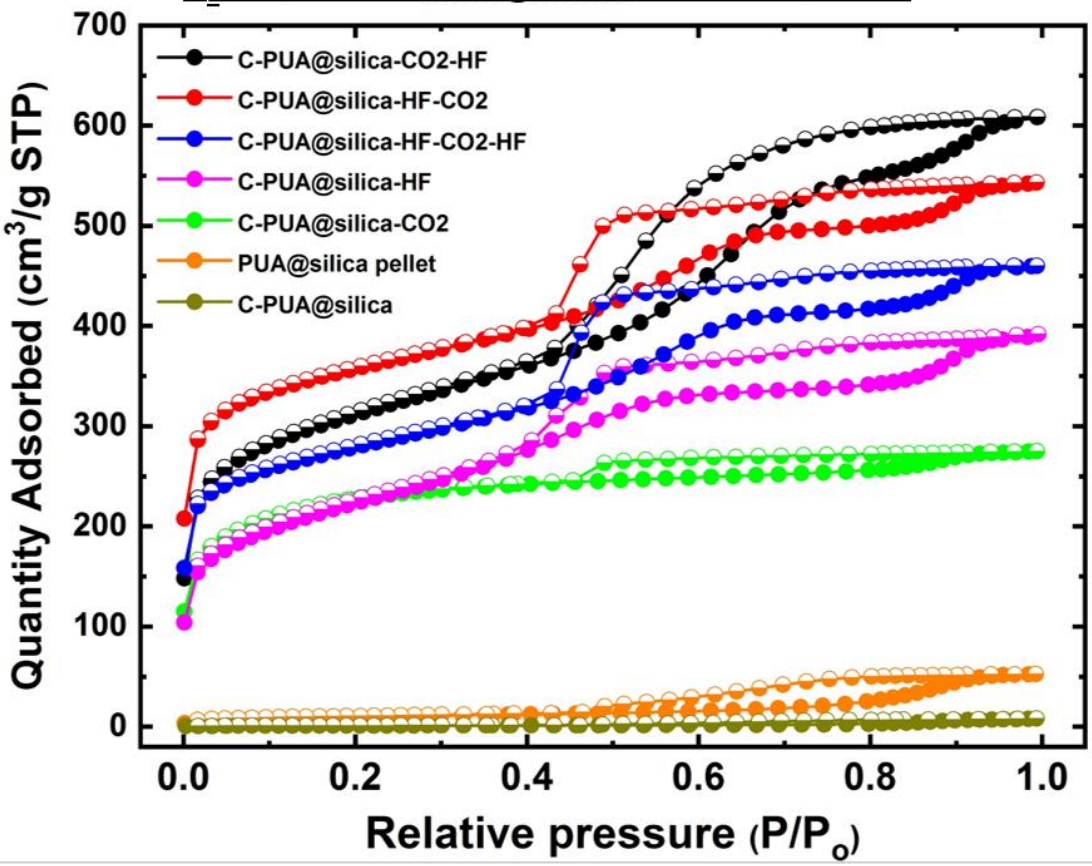

PAN@silica (TMOS:APTES = 90:10) 60% AN crosslinked

sample I.D.	linear shrinkage[a,b] (%)	bulk density[a], ρ_b (g cm^{-3})	skeletal density[c], ρ_s (g cm^{-3})	porosity[d], Π (% v/v)	mass loss[a], (% w/w)	specific pore volume (cm^3 g^{-1})			BET surface area[h], σ (m^2 g^{-1})	avg pore diameter[i], Φ (nm)
						V_{Total}[e]	$V_{1.7\text{-}300\ nm}$[f]	$V_{>300\ nm}$[g]		
PAN@silica compact		1.1016 ± 0.0296	1.2229 ± 0.0029	9.92%		0.09	0.02	0.07	2.31 [1.24]	155 [28.79]
aromatized-PAN@silica	12.01 ± 1.38 %	1.3069 ± 0.0133	1.5037 ± 0.0022	13.06%	11.87 ± 0.89 %	0.10	0.00	0.10	0.13 [0.16]	3046 [19.41]
C-PAN@silica	26.78 ± 1.01 %	1.3342 ± 0.0224	1.8326 ± 0.0205	27.20%	35.98 ± 1.58 %	0.20	0.00	0.20	0.03 [0.48]	31726 [45.29]
C-PAN@silica-HF	26.45 ± 0.34 %	1.1348 ± 0.0108	1.7595 ± 0.0094	35.50%	46.96 ± 0.77 %	0.31	0.09	0.23	131 [2.63]	9.55 [3.92]
C-PAN@silica-HF-CO_2	33.72 ± 2.16 %	0.7101 ± 0.0279	1.8783 ± 0.0181	62.19%	72.74 ± 0.49 %	0.88	0.29	0.58	864 [483]	4.05 [2.87]
C-PAN@silica-HF-CO_2-HF	33.29 ± 1.07 %	0.8612 ± 0.0478	1.7947 ± 0.0078	52.01%	67.52 ± 2.34 %	0.60	0.25	0.35	611 [326]	3.95 [3.00]
C-PAN@silica-CO_2	37.54 ± 1.38 %	1.1059 ± 0.0177	2.1323 ± 0.0130	48.14%	60.05 ± 0.93 %	0.44	0.01	0.43	441 [347]	3.95 [2.07]
C-PAN@silica-CO_2-HF	38.12 ± 2.35 %	0.7783 ± 0.0554	1.7986 ± 0.0008	56.73%	72.21 ± 2.23 %	1.24	0.21	1.03	630 [322]	7.86 [2.88]

N_2 sorption for PAN@silica processed pellets

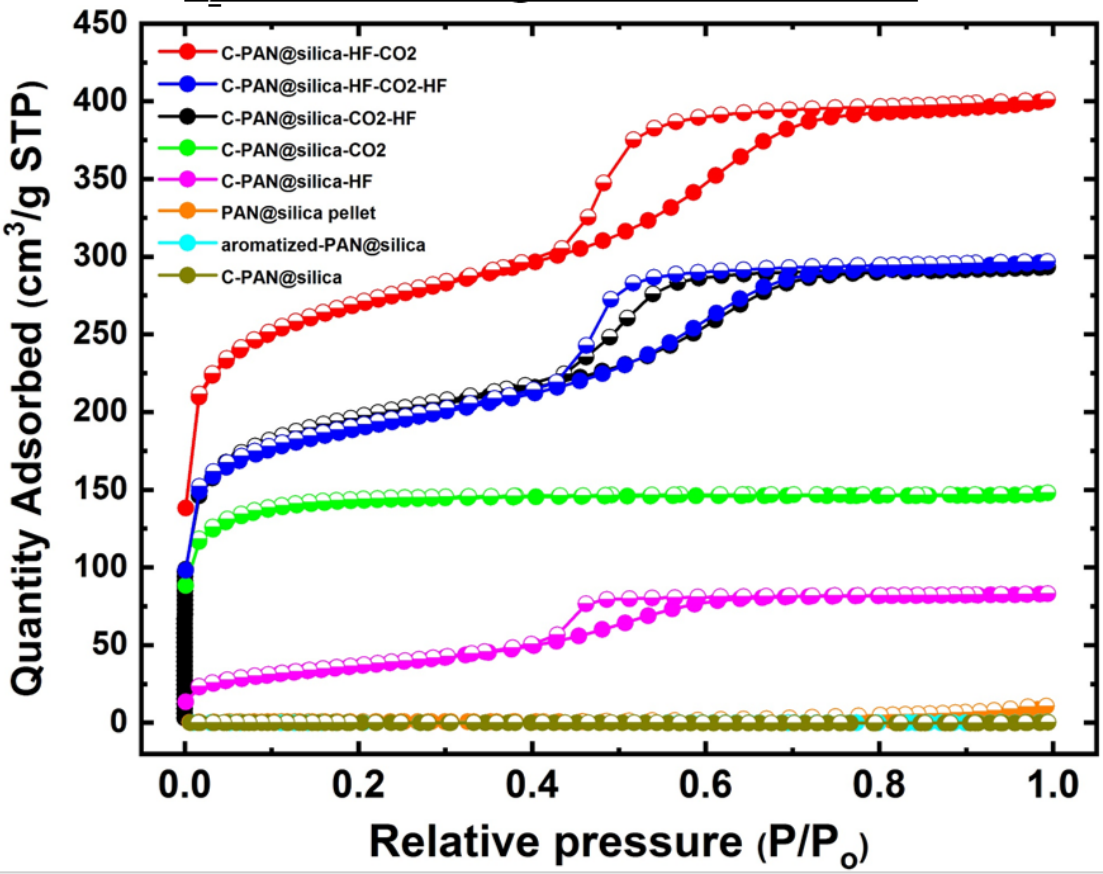

PAN@silica (TMOS:APTES = 90:10) 30% AN crosslinked

sample I.D.	linear shrinkage (%)	bulk density, ρ_b (g cm^{-3})	skeletal density, ρ_s (g cm^{-3})	porosity, Π (% v/v)	yield (% w/w)	mass loss (% w/w)	specific pore volume (cm^3 g^{-1})			BET surface area, σ (m^2 g^{-1})	avg pore diameter Φ (nm)
							V_{Total}	$V_{1.7\text{-}300\ nm}$	$V_{>300\ nm}$		
PAN@silica compact		1.1222 ± 0.0142	1.1821 ± 0.0019	5.07%							
PAN@silica-aromatized	8.52 ± 0.45 %	1.2087 ± 0.0113	1.5544 ± 0.0052	22.24%	90.87 ± 1.04 %	9.13 ± 1.04 %					
C-PAN@silica	22.52 ± 0.66 %	1.2619 ± 0.0162	1.8513 ± 0.0191	31.84%	65.12 ± 1.04 %	34.88 ± 1.04 %					
C-PAN@silica-HF	24.16 ± 0.56 %	1.0196 ± 0.0034	1.7798 ± 0.0062	42.71%	52.10 ± 0.63 %	47.90 ± 0.63 %					
C-PAN@silica-HF-CO_2	37.32 ± 0.31 %	0.4108 ± 0.0215	1.8138 ± 0.0399	77.35%	13.02 ± 0.52 %	86.98 ± 0.52 %	1.88	1.36	0.52	1141 [332]	6.60 [5.38]
C-PAN@silica-HF-CO_2-HF	37.41 ± 0.55 %	0.4375 ± 0.0265	2.0468 ± 0.0327	78.63%	13.83 ± 0.99 %	86.17 ± 0.99 %	1.80	1.39	0.41	1042 [258]	6.90 [5.80]
C-PAN@silica-CO_2	31.19 ± 0.93 %	1.1766 ± 0.0294	2.0326 ± 0.0071	42.11%	50.58 ± 0.42 %	49.42 ± 0.42 %					
C-PAN@silica-CO_2-HF											

PAN@silica (TMOS:APTES = 70:30) 60% AN crosslinked (new batch)

sample I.D.	linear shrinkage (%)	bulk density, ρ_b (g cm^{-3})	skeletal density, ρ_s (g cm^{-3})	porosity, Π (% v/v)	yield (% w/w)	mass loss (% w/w)	specific pore volume (cm^3 g^{-1})			BET surface area, σ (m^2 g^{-1})	avg pore diameter Φ (nm)
							V_{Total}	$V_{1.7\text{-}300\ nm}$	$V_{>300\ nm}$		
PAN@silica compact		1.1195 ± 0.0173	1.2585 ± 0.0014	11.04 %							
PAN@silica-aromatized	13.64 ± 0.91 %	1.2802 ± 0.0150	1.6042 ± 0.0018	20.20 %	85.04 ± 1.46 %	14.96 ± 1.46 %					
C-PAN@silica	29.18 ± 1.35 %	1.3057 ± 0.0248	1.9147 ± 0.0154	31.81 %	59.09 ± 1.89 %	40.91 ± 1.89 %					
C-PAN@silica-HF											
C-PAN@silica-HF-CO_2											
C-PAN@silica-HF-CO_2-HF											
C-PAN@silica-CO_2											
C-PAN@silica-CO_2-HF											

Solid Framework Characterization. Scanning electron microscopy (SEM) was conducted with Au, Pd-coated samples on a Hitachi Model S-4700 field-emission microscope.

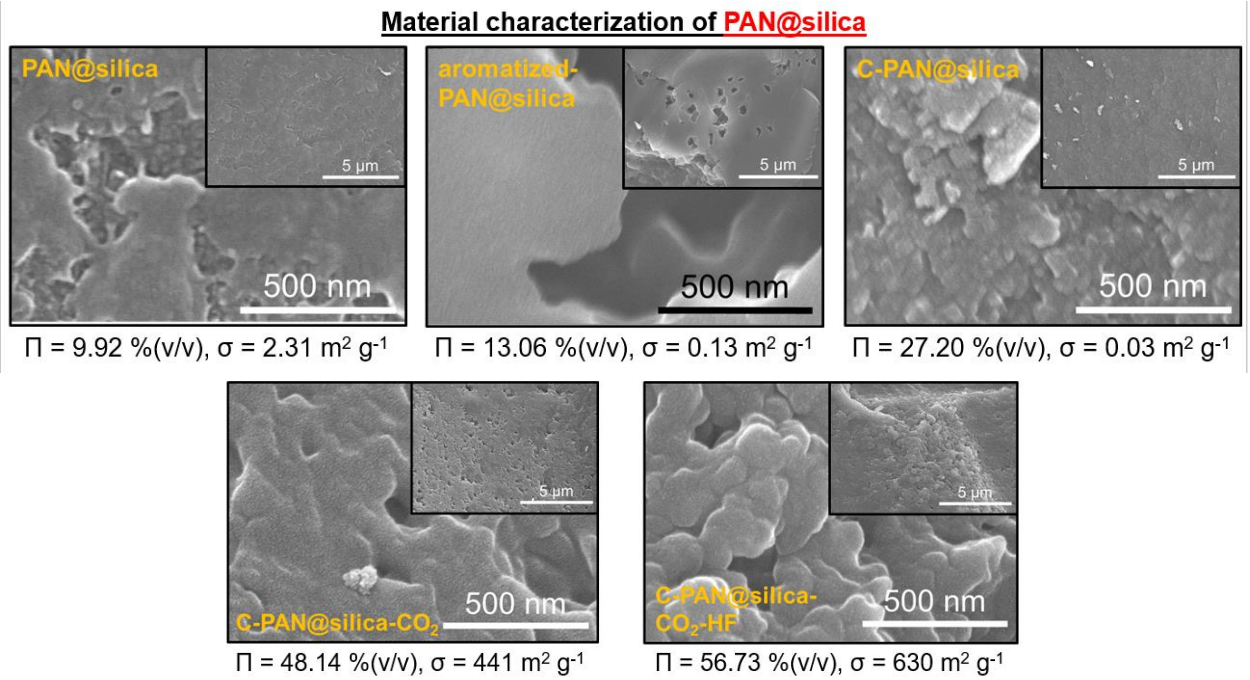

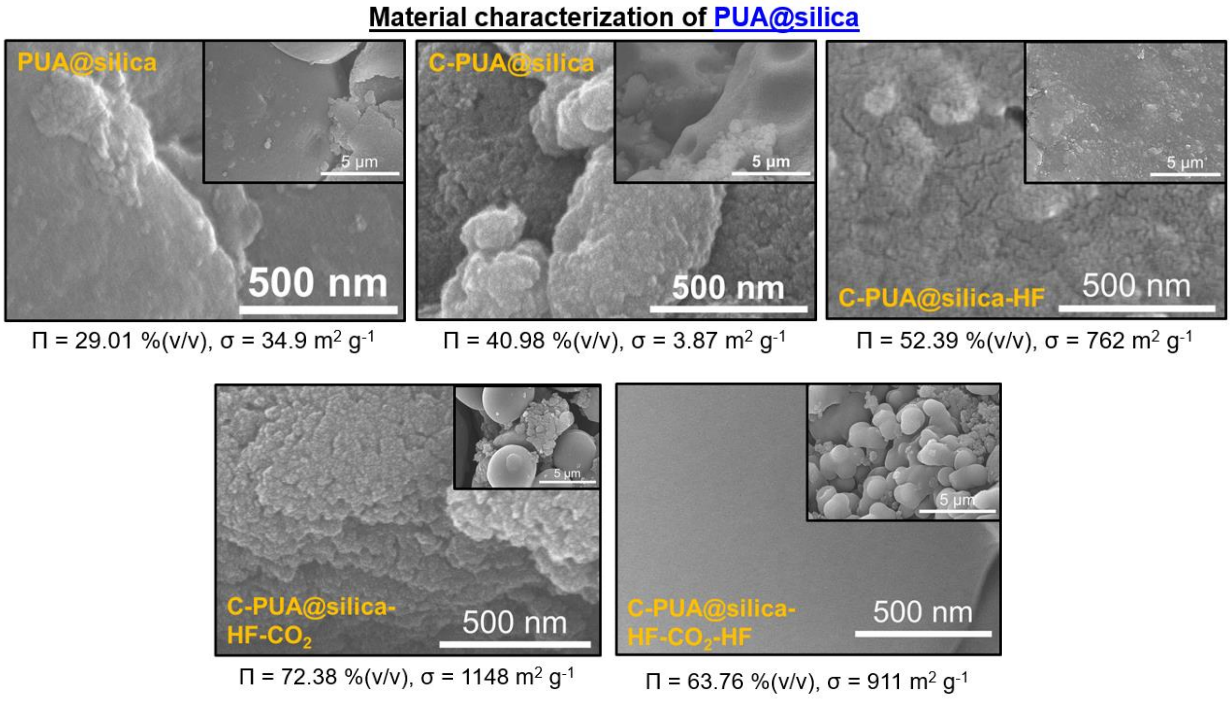

Material characterization of PUA@silica

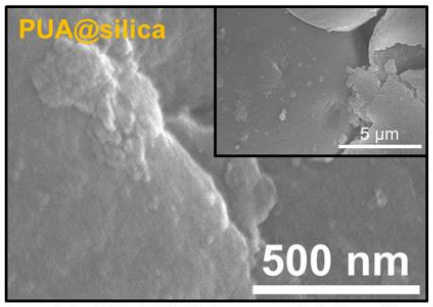

Π = 29.01 %(v/v), σ = 34.9 m^2 g^{-1}

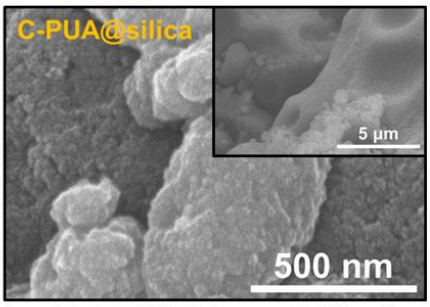

Π = 40.98 %(v/v), σ = 3.87 m^2 g^{-1}

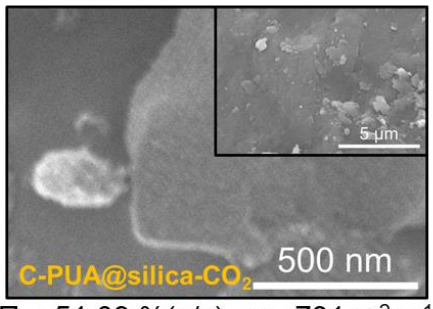

Π = 51.09 %(v/v), σ = 731 m^2 g^{-1}

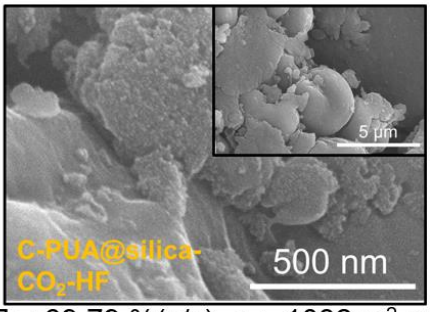

Π = 69.79 %(v/v), σ = 1032 m^2 g^{-1}

Material characterization of PAN@silica

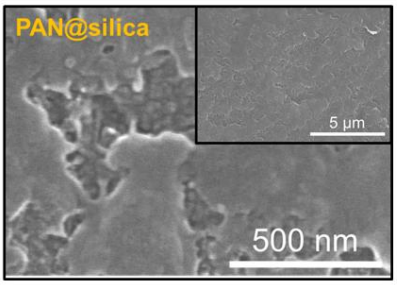

Π = 9.92 %(v/v), σ = 2.31 m^2 g^{-1}

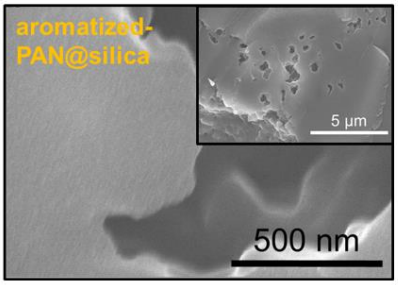

Π = 13.06 %(v/v), σ = 0.13 m^2 g^{-1}

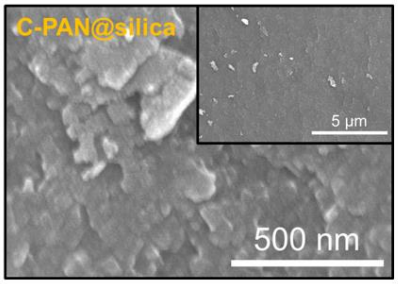

Π = 27.20 %(v/v), σ = 0.03 m^2 g^{-1}

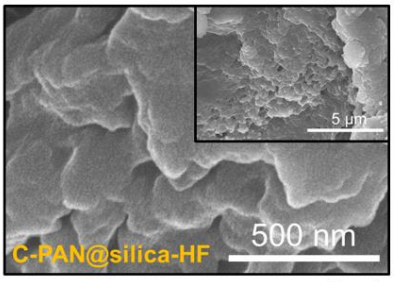

Π = 35.50 %(v/v), σ = 131 m^2 g^{-1}

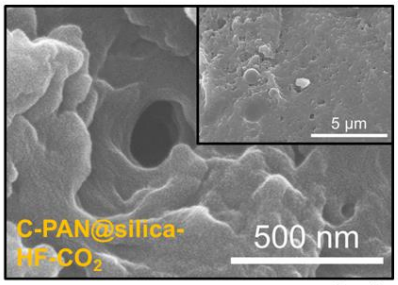

Π = 62.19 %(v/v), σ = 864 m^2 g^{-1}

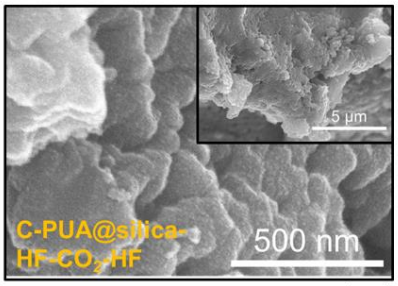

Π = 52.01 %(v/v), σ = 611 m^2 g^{-1}

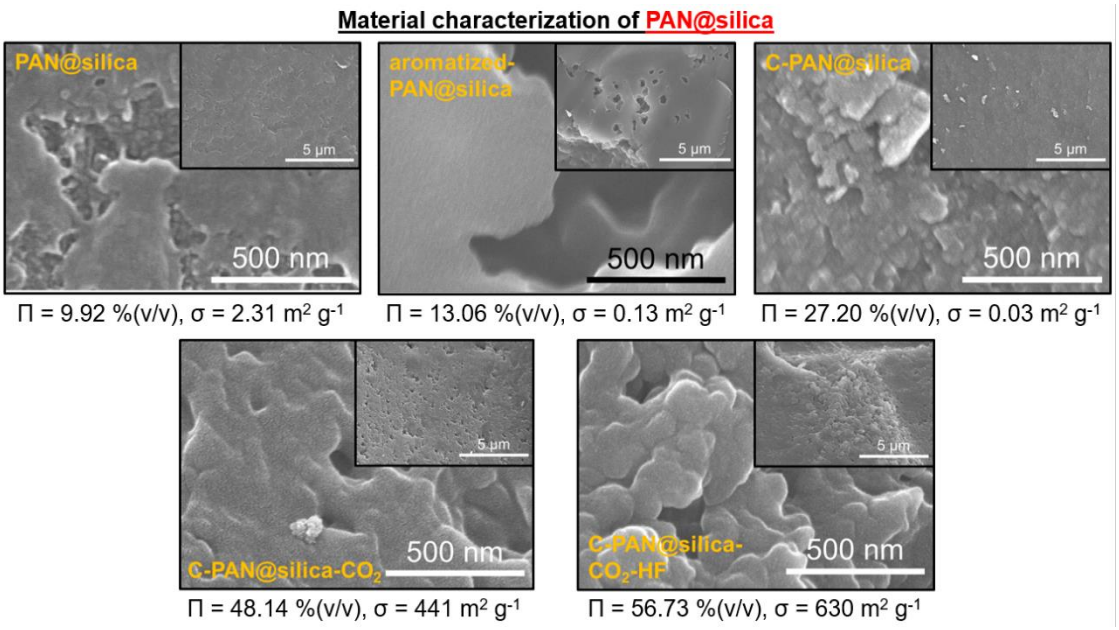

Quantitative Characterization. Thermogravimetric analysis (TGA) was conducted under O_2 with a TA Instruments Model TGA Q50 thermogravimetric analyzer, using a heating rate of 5°C min^{-1}. Modulated Differential Scanning Calorimetry (MDSC) was conducted under O_2 with a TA Instruments Differential Scanning Calorimeter Model Q2000, using a heating rate of 10°C min^{-1}.

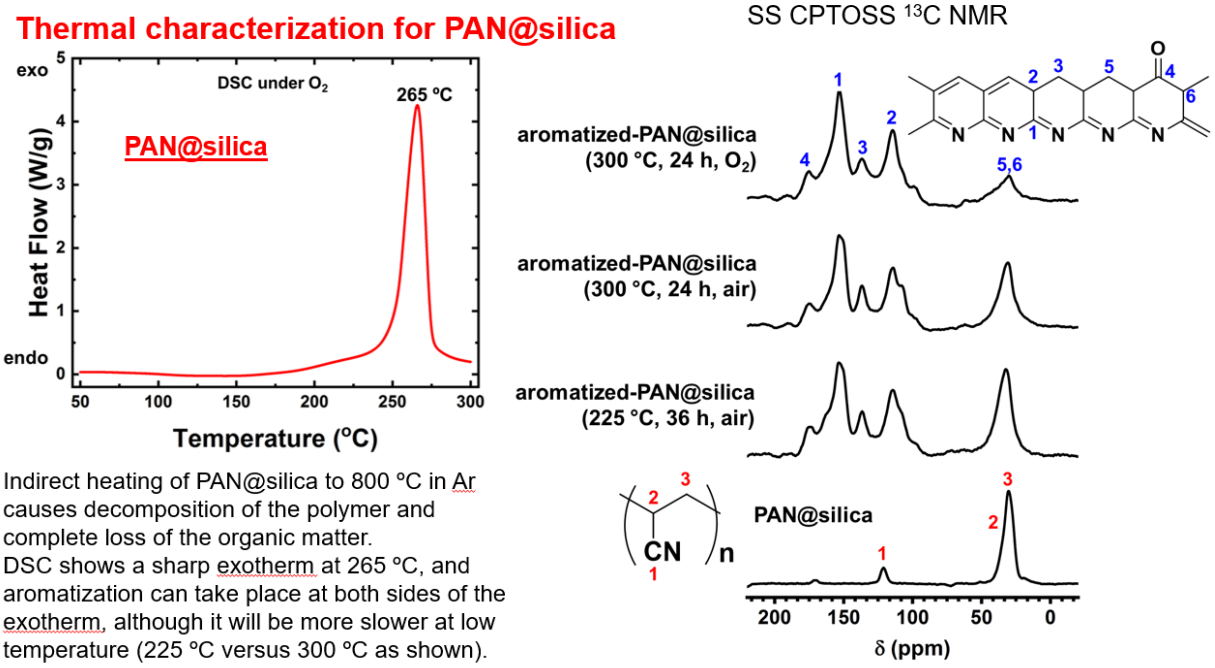

Indirect heating of PAN@silica to 800 °C in Ar causes decomposition of the polymer and complete loss of the organic matter.
DSC shows a sharp exotherm at 265 °C, and aromatization can take place at both sides of the exotherm, although it will be more slower at low temperature (225 °C versus 300 °C as shown).

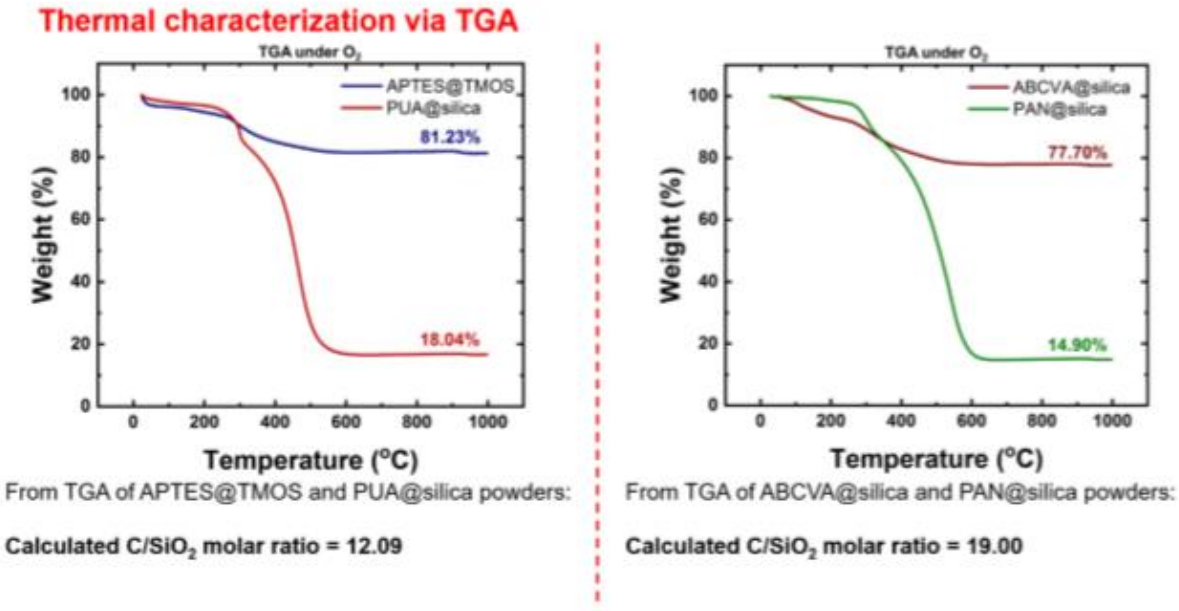

Future Research. Currently, the characterization of the PAN@silica (TMOS: APTES = 90:10) with 30% AN crosslinking and the PAN@silica (TMOS: APTES = 70:30) with 60% AN crosslinking is being determined. After that is finished, the new batch of PAN@silica (TMOS:APTES = 70:30) with 30% AN will be processed. Also, the PUA@silica with 2x TIPM and 1x TIPM will be processed. A 6x TIPM PUA@silica will be made if necessary.

Acknowledgements:

I would like to thank my research advisor Chariklia Sotiriou-Leventis and the research group for helping me with this project.

References:

1. Antonietti, M.; Fechler, N.; Fellinger, T.-P. Carbon Aerogels and Monoliths: Control of Porosity and Nanoarchitecture via Sol–Gel routes. *Chem. Mater.* **2014**, *26*, 196–210.

2. Majedi Far, H.; Rewatkar, P. M.; Donthula, S.; Taghvaee, T.; Malik Saeed, A.; Sotiriou-Leventis, C.; Leventis, N. Exceptionally High CO_2 Adsorption at 273 K by Microporous Carbons from Phenolic Aerogels: The Role of Heteroatoms in Comparison with Carbons from Polybenzoxazine and Other Organic Aerogels. *Macromol. Chem. Phys.* **2018**, *220*, 1800333.

3. Pierre, A. C.; Pajonk, G. M. Chemistry of Aerogels and Their Applications. *Chem. Rev.* **2002**, *102*, 4243−4265.

4. Rewatkar, P. M.; Taghvaee, T.; Saeed, A. M.; Donthula, S.; Mandal, C.; Chandrasekaran, N.; Leventis, T.; Shruthi, T. K.; Sotiriou-Leventis, C.; Leventis, N. Sturdy, Monolithic SiC and Si3N4 Aerogels from Compressed Polymer-Cross-Linked Silica Xerogel Powders. *Chem. Mater.* **2018**, 30, 1635-1647.

5. Leventis, N.; Chandrasekaran, N.; Sotiriou-Leventis, C.; Mumtaz, A. "Smelting in the age of nano: Iron aerogels," J. Mater. Chem. 2009, 19, 63-65.

6. Leventis, N.; Chandrasekaran, N.; Sadekar, A. G.; Mulik, S.; Sotiriou-Leventis, C. "The effect of compactness on the carbothermal conversion of interpenetrating metal oxide / resorcinolformaldehyde nanoparticle networks to porous metals and carbides," J. Mater. Chem. 2010, 20, 7456-7471.

7. Leventis, N.; Sotiriou-Leventis, C.; Chandrasekaran, N.; Mulik, S.; Larimore, Z. J.; Lu, H.; Churu, G.; Mang, J. T. "Multifunctional polyurea aerogels from isocyanates and water. A structure-property case study," Chem. Mater. 2010, 22, 6692-6710.

8. Sadekar, A. G.; Mahadik, S. S.; Bang, A. N.; Larimore, Z. J.; Wisner, C. A.; Bertino, M. F.; Kalkan, A. K.; Mang, J. T.; Sotiriou-Leventis, C.; Leventis, N. "′Green′ aerogels and porous carbons by emulsion gelation of acrylonitrile," Chem. Mater. 2012, 24, 26-47.

9. Mahadik-Khanolkar, S.; Donthula, S.; Bang, A.; Wisner, C.; Sotiriou-Leventis, C.; Leventis, N. "Polybenzoxazine aerogels. 2. Interpenetrating networks with iron oxide and the carbothermal synthesis of highly porous monolithic pure iron(0) aerogels as energetic materials," Chem. Mater. 2014, 26, 1318-1331.